PHYSICAL REVIEW E **72**, 025602(R) (2005)

Non-Gaussian statistics of optical near-fields

A. Apostol and A. Dogariu
College of Optics and Photonics/CREOL, University of Central Florida, Orlando, FL 32816, USA
(Received 1 November 2004; revised manuscript received 17 February 2005; published 18 August 2005)

Optical fields in the proximity of random media can be modeled as a superposition of waves with random phases. We demonstrate that, depending on the experimental geometry, both Gaussian and non-Gaussian regimes can be established for the statistics of scattered intensity. In a reflection-emission configuration, the first-order statistics of the scattered light is non-Gaussian and it can be used to retrieve information about the physical interface.

DOI: 10.1103/PhysRevE.72.025602 PACS number(s): 42.25.Dd, 42.25.Kb, 05.40.Fb

The optical near-fields generated in the proximity of randomly inhomogeneous media are usually contributions of both propagating and evanescent components. Their occurrence may be due to either global or local excitation of the inhomogeneous medium and, in this paper, we will show that depending upon the type of excitation, different statistical manifestations of the properties of optical fields are obtained. When a random interference pattern is produced by overlapping harmonic waves having random phases, the process can be modeled as a typical two-dimensional (2D) random walk problem [1]. This concept has described successfully a number of optical phenomena obeying both Gaussian and non-Gaussian statistics [1–3]. In the case of quasimonochromatic radiation, the intensity probability density function is evaluated by considering the stochastic process to be a random walk in the complex plane. The approach has been used to describe the formation of the far-field speckles but it can also be applied in the near-field, where the evanescent field components contribute to the statistical properties of the intensity distribution.

Near-field speckles can be produced as a result of the global excitation of a random medium. This is the case of the transmission-collection configuration illustrated in the inset of Fig. 1 where radiation from a light source propagates through a random medium and is collected close to the surface by an optical probe. In practice, an Arion laser ($\lambda = 488$ nm) is used to illuminate an area of 300×300 μm on the bottom surface of an optically thick medium and the transmitted field is coupled to the cantilevered near-field optical sensor while the tip is scanned along the sample. The scattered light is detected by a photomultiplier tube operating in photon counting mode. The near-field scanning optical microscope (NSOM) [4] allows obtaining simultaneously the near-field optical images and the corresponding atomic force microscope (AFM) topographical images. The Al-coated fused silica fiber tip with an aperture of 150 nm provides the possibility to scan in constant distance mode.

In the close vicinity of the surface, the tip collects both propagating and evanescent components of the emitted field. At a given observation point, the field is a superposition of a large number of contributions originating from different locations within the bulk; the amplitude and the phase of the elementary scattering centers satisfy the requirements of circular Gaussian statistics. As seen in Fig. 1, this is confirmed by the first-order statistics of intensity; the measured probability density function $p(I)$ obeys a negative exponential and, therefore, the corresponding optical contrast, $\sqrt{(\langle I^2\rangle - \langle I\rangle^2)}/\langle I\rangle$, is close to unity. The data analyzed here correspond to slabs of calcium carbonate and kaolin microparticles having a large size distribution, but similar behavior has been observed for a variety of optically thick random media. The slabs are compacted and their optical density is higher than ten, i.e., light propagates at least ten transport mean free path before being transmitted through the random medium. The data presented in Fig. 1 are collected on such a compacted slab with r.m.s roughness of 92 nm. The same behavior of the intensity distribution was also obtained for other media having the r.m.s. fluctuations of the surface height ranging between $\lambda/40$ and $\lambda/2$. In the present case, the strong multiple scattering in the bulk distributes uniformly the phases of the elementary scattering centers. Multiple scattering also increases the number of field contributions at any examined point, irrespective of the values of the r.m.s. fluctuations of surface height. In addition, the amplitudes and the phases of the field originating from a large number of elementary scattering centers are statistically independent random variables. As a consequence of all these, the real and imaginary parts of the complex scattered field obey circular Gaussian statistics and the amplitude of the

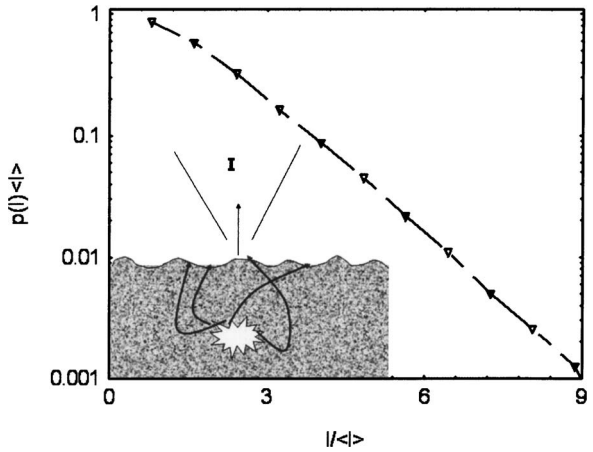

FIG. 1. Transmission-collection configuration for global excitation of a random medium and the corresponding normalized intensity probability density. The inset depicts this mode of operation.

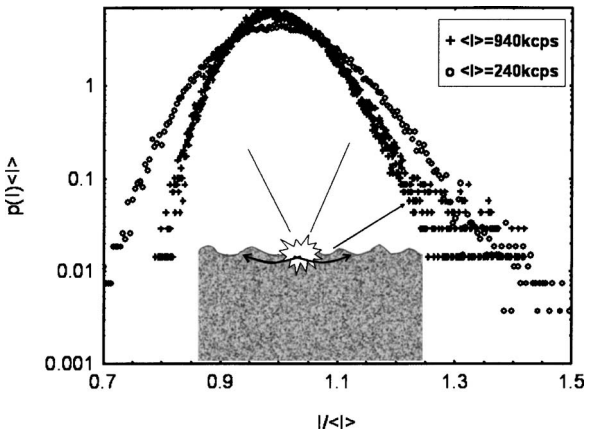

FIG. 2. Emission-reflection configuration for local excitation of a random medium and the corresponding normalized intensity probability density. Experimental results are shown for different average intensities as indicated. The inset depicts this mode of operation.

resultant field has a Rayleigh distribution [5,6].

A local excitation of a random medium may occur, for instance, when the medium is illuminated with an NSOM tip as illustrated in the inset of Fig. 2. In this emission-reflection configuration, the light is coupled to one end of the fiber and the radiation emanates from the other end that is tapered down to a diameter of 100 nm. In the configuration of Fig. 2, the radiation is coupled onto the medium which contains subwavelength variations in both the topography and its optical properties, and is then re-emitted in the form of a scattered field.

During the scattering process, some of the evanescent components are being converted into propagating waves, which are then detected in the far field by a 50× magnification microscope objective (0.45 NA) with a 13.8 mm working distance and imaged onto an avalanche photodiode (SPCM-200; EG&G). This collection system determines on the surface of the sample a collection area of approximately 300 μm^2. As in the previous case, the NSOM probe can be scanned in constant distance mode and permits obtaining simultaneously the AFM topography and the distribution of intensities.

As opposed to the global excitation case, the intensity probability density function is not a negative exponential anymore. Measurements in this configuration were performed on similar slabs of calcium carbonate and kaolin microparticles which were compacted such that they generate pores with a size distribution centered at 20 nm as determined by the mercury porosimetry. The samples are optically opaque, their thickness is 1 mm and the scattering mean free path is approximately 100 μm. One should notice that the value of the scattering mean free path is significantly larger than the 20 μm diameter of the collection area which is determined by the optical system. In all cases examined, the absorption was negligible.

It is evident that, when the random medium is locally illuminated by the tip, the resultant intensity statistics has a non-Gaussian behavior. This regime is generated when, at a given observation point, the field is the result of the superposition of a limited number of contributions originating from different locations within the random medium. Non-Gaussian statistics may also be the result of weak scattering, when the phases of the elementary scattering centers are no longer uniformly distributed. This happens when the probability density function of their phases depends on the surface statistics or when there is a certain correlation between the superposing waves which form the speckle pattern.

In Fig. 2 we present the measured probability density function $p(I)$ obtained by scanning the surface of a compact slab having the same r.m.s height fluctuations of 92 nm as the one in Fig. 1. When examining the data, an interesting observation can be made. The intensity probability density function depends on the measured average intensity, which can be adjusted by changing the incident intensity coupled into the fiber tip. Such a dependence of the statistical properties of the scattered field on the excitation level could not be observed in any of the transmission measurements. The change of the intensity statistics, when the incident intensity is increased, is somewhat puzzling because one should not expect any nonlinear phenomena in the media examined. This behavior can be explained by realizing that (i) the radiation couples onto the medium away from the tip before being re-emitted, and (ii) the noise level of the light detection process imposes an inherent intensity cutoff. As a result, when the intensity coupled into the medium increases, the detection system collects radiation from a larger area on the surface of the medium changing the statistical properties of the detected radiation, as will be explained in the following.

For all practical proposes, a simple model can be developed by considering that due to inhomogeneities in the optical properties, the light is first coupled inside the medium over a surface of area A, the size of which depends on the incident intensity. Within this area, N independent elementary scattering centers are being excited. In a first approximation, one can further consider that A is proportional with the incident intensity, and so is N. We can regard these elementary scattering centers as being distributed on the physical interface of the random medium.

Due to the coupling of radiation onto the medium, the elementary scattering centers are not excited in phase; the distribution of their initial phase θ_i is determined by the local properties of the medium. For simplicity, one can consider the probability density of the initial phase of these elementary scattering centers to be a Gaussian $(1/\sqrt{2\pi}\Delta\theta_i)^{-1/2}\exp[-(\theta_i/2\Delta\theta_i)^2]$ with the r.m.s fluctuations $\Delta\theta_i$ depending on the local characteristics of the inhomogeneous medium.

The radiation re-emitted by the N elementary scattering centers is then collected in the far-field, after accumulating an additional phase θ_p, depending on the distribution of the surface heights. When the excited regions are larger than the lateral correlation area of the surface, the surface statistics is stationary over areas of size A. As the heights of the interface are Gaussian distributed, so will be the additional phases θ_p of the emitted field. The r.m.s fluctuations of this phase are determined by the surface roughness, $\Delta\theta_p = k_o\sigma$, where k_o is the wave number in air and σ represents the r.m.s height of the surface fluctuations. If the phases θ_i and θ_p are statistically independent random variables, the distribution of the total phase of the elementary scattering centers, $\theta = \theta_i + \theta_p$, is also a Gaussian function with the r.m.s fluctuations being $\Delta\theta = \sqrt{\Delta\theta_i^2 + \Delta\theta_p^2}$.

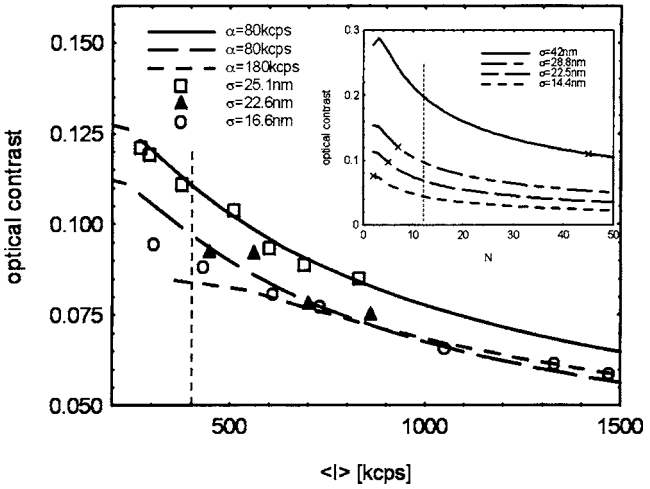

FIG. 3. Dependence of the optical contrast on the average intensity for different r.m.s. roughness of the surface as indicated. The symbols represent typical experimental results, while the curves are the theoretical predictions based on the random walk model of Ref. [8] evaluated for $\Delta\theta_i=0.268$ rad. The inset shows the optical contrast as a function of the number N of elementary scattering centers for different values of the surface roughness. The crosses denote the experimental values of the contrast and the corresponding values of N for an average intensity of 400 kcps which is indicated by the vertical dotted line in the main figure.

The situation can now be regarded as a coherent superposition of waves scattered by N independent but identical elementary scattering centers and can be described as a random walk in the complex space. The amplitude and the phases of the field emitted by the elementary scattering centers are statistically independent random variables. However, as opposed to the transmission-collection configuration, their phases are no longer uniformly distributed. The probability density function of their phases is approximated by a Gaussian distribution with the r.m.s phase fluctuations $\Delta\theta$ determined by both surface ($\Delta\theta_p$) and subsurface ($\Delta\theta_i$) properties of the inhomogeneous medium.

The coherent superposition of the waves forms a speckle pattern whose intensity statistics depends on their number N and on their phase distributions [7–9]. For a given phase distribution, Barakat has shown that the optical contrast can actually decrease when the number of independent contributions increases [8]. This is illustrated in the inset of Fig. 3 where the optical contrast of this random interference is evaluated for different phase distributions of the scattering centers: $\Delta\theta=\sqrt{\Delta\theta_i^2+\Delta\theta_p^2}$. The calculations are for $\Delta\theta_i=0.268$ rad and $\Delta\theta_p=k_o\sigma$, each curve corresponding to a surface with a roughness σ as indicated. One can notice that, for a given value of N, the random walk model leads to an increase of the optical contrast with the roughness of the interface; this happens, for instance, along the dotted vertical line in the inset of Fig. 3.

We would like to emphasize that the same random walk model can also explain the case when the phases of the elementary scattering centers are uniformly distributed. In this Gaussian regime, the optical contrast increases with N and very quickly reaches the saturation value of unity. It is important to realize that it is not only the number of the scattering centers which governs the non-Gaussian regime of the random interference but also the departure of the phase from being uniformly distributed.

The simple model outlined above makes a good description of the experimental results. Typical values of the measured optical contrast are shown in Fig. 3 for different surface roughness and for different average intensities, which were adjusted by modifying the excitation level. The data were recorded over areas of 5×5 μm situated at the same distance z from the surface. In order to explain the experimental data, let us consider that the average intensity $\langle I\rangle$ over the scanning area is proportional with the incident intensity or, in other words, with the number of elementary scattering centers $\langle I\rangle=\alpha N$. Note that even if the number N of the elementary scattering centers increases when the excitation level increases, their phase distribution does not necessarily change. This is a consequence of the fact that the effective local properties of the medium are the same irrespective of the size of the illuminated area.

In Fig. 3, each curve is evaluated using the model previously outlined for a certain value of the coupling parameter α and for a Gaussian phase distribution with the width $\Delta\theta=\sqrt{\Delta\theta_i^2+\Delta\theta_p^2}$. In this evaluation, we used (i) $\Delta\theta_p=k_o\sigma$ with σ being the measured AFM roughness of the scanned area, and (ii) $\Delta\theta_i=0.268$ rad, which was found to best fit all the experimental data collected on surfaces with different r.m.s. height fluctuations. This value of $\Delta\theta_i$ should relate to the local fluctuations of the dielectric constant and is therefore material dependent. The relation between the initial phase distribution of the elementary scattering centers and the local characteristics of the inhomogeneous medium can be established based on a microscopic model of the local dielectric function. For the purpose of our discussion, however, it is important to realize that the constant value of $\Delta\theta_i$ reflects the fact that the local optical properties are independent not only of the size of the illuminated area but also of the surface roughness. As previously pointed out, the simple model of the coherent superposition of waves allows for both surface ($\Delta\theta_p$) and subsurface ($\Delta\theta_i$) effects to be accounted for.

The number N of elementary scattering centers can now be inferred using the fitting procedure illustrated in Fig. 3. For instance, the crosses in the inset of Fig. 3 indicate the experimental values of the optical contrast and of the corresponding number N obtained for an average intensity of 400 kcps (the vertical dotted line in Fig. 3) and for different values of the surface roughness.

Using the data analysis presented above, the statistical properties of the optical radiation can be related to the statistical properties of the surface. The dependence of the optical contrast on the surface roughness is shown in Fig. 4 where the experimental results correspond to an average intensity of 400 kcps. The curves are the predictions of the random walk model evaluated for $\Delta\theta_i=0.268$ rad, $\Delta\theta_p=k_o\sigma$, and for the number of elementary scattering centers N estimated from the fitting procedure illustrated in Fig. 3. We remark that, for relatively smooth surfaces, the non-Gaussian near-fields have an optical contrast which increases with the r.m.s roughness of the physical interface. It is also interesting

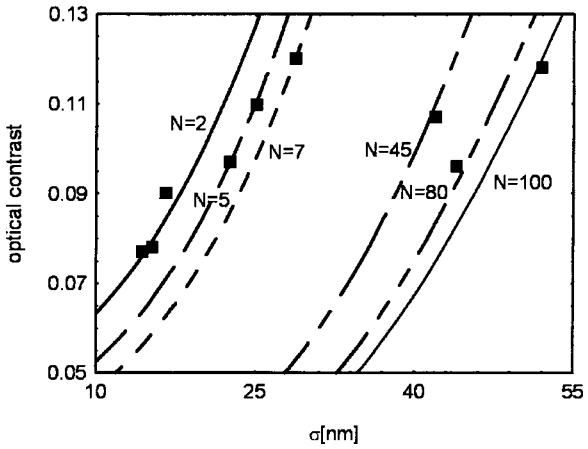

FIG. 4. Dependence of the optical contrast on the surface roughness. The symbols denote the experimental results measured for an average intensity $\langle I \rangle = 400$ kcps while the curves represent the predictions of the random walk model for $\Delta\theta_i = 0.268$ rad and $\Delta\theta_p = k_o\sigma$.

to note that, when the surface becomes rougher, more independent scattering centers tend to contribute to the detected intensity. However, the intensity distribution is still non-Gaussian because the phases of the elementary scattering centers are not uniformly distributed.

In conclusion, we have shown that fluctuating optical fields in the neighborhood of a random medium can exhibit either Gaussian or non-Gaussian statistics. Different regimes are obtained as a result of specific experimental configurations for exciting the highly inhomogeneous media.

In the situation when a global excitation is applied, such as in a transmission-collection geometry of an NSOM, the intensity variations in the near-field satisfy the requirements of circular Gaussian statistics. The multiple scattering in the bulk completely randomizes the phases and a large number of independent scattering centers contribute to the field in each speckle point. As a result, the intensity probability density function has a negative exponential dependence, and the contrast is always close to unity. In this case, when light is transmitted through or is emitted within a highly scattering medium, the first-order statistics of intensity cannot be used to infer information about the surface.

However, when randomly inhomogeneous media are excited locally, in an emission-reflection geometry, for example, we found that the near-field speckle patterns are governed by non-Gaussian statistics and, consequently, the optical contrast is significantly smaller than unity. We have shown that, in practice, the probability density of the scattered intensity depends on the physical properties of the interface and also on the incident light intensity. We have demonstrated that, in this situation, the stochastic properties of the scattered intensity can be used to determine the statistical properties of the physical surface.

When the experimental configuration is properly accounted for, a simple model considering the superposition of waves having random phases can describe both statistical regimes encountered in the near-field of random media. As illustrated in this study, understanding the random interference phenomena in the near-field could lead to new possibilities for surface and subsurface diagnostics of inhomogeneous media.

[1] *Laser Speckle and Related Phenomena* (J. C. Dainty, New York, 1975).
[2] P. Pusey, *Photon Correlation and Velocimetry* (H. Z. Cummins and G. R. Pike, New York, 1977).
[3] E. Jakeman and R. Tough, Adv. Phys. **37**, 471 (1988).
[4] K. Lieberman, N. Ben-Ami, and A. Lewis, Rev. Sci. Instrum. **67**, 3567 (1996).
[5] A. Apostol and A. Dogariu, Phys. Rev. Lett. **91**, 093901 (2003).
[6] A. Apostol and A. Dogariu, Opt. Lett. **29**, 235 (2004).
[7] J. Uozumi and T. Asakura, Atti Fond. Giorgio Ronchi **25**, 537 (1977).
[8] Richard Barakat, J. Opt. Soc. Am. **71**, 86 (1981).
[9] J. Uozumi and T. Asakura, J. Opt. **12**, 177 (1981).